

STRESS- AND STRAIN-BASED FATIGUE LIFE CALCULATION FOR SHORT FIBER REINFORCED POLYMERS BY USE OF FE-SAFE®

D. Kaylani^{1*}, A. Primetzhofer¹, G. Stadler², T. Zacharias³, T. Toenz³ and G. Pinter²

¹ Polymer Competence Center Leoben GmbH, Leoben, Austria,

² Materials Science and Testing of Polymers, Montanuniversitaet Leoben, Leoben, Austria,

³ medmix Switzerland AG, Haag, Switzerland

* dario.kaylani@pccl.at

Keywords: fatigue, simulation, short-fiber-reinforced polymers, fe-safe

1 INTRODUCTION

Components subjected to mechanical stresses are increasingly manufactured from short fiber reinforced thermoplastic polymers (SFRPs). These materials feature high strength and cost-efficient manufacturing possibilities, meeting increasing demands in terms of emission reduction, material utilization and lightweight construction. The material behavior of fiber reinforced thermoplastics under cyclic loading strongly depends on process- and environment related influence factors. Local fiber orientation has a significant impact on the mechanical material properties [1–3]. Established methods must therefore be extended to cover these effects and account for varying mechanical and fatigue properties throughout the structure. To cover one of the most pronounced influencing factors regarding the fatigue life of SFRPs, a continuous simulation chain must include process simulation, anisotropic stress calculation by FEA and fatigue life calculation. Starting with an injection molding simulation, the local fiber orientation can be predicted and transferred to a lifetime assessment alongside the results from a structural analysis. Contrary to other recent work associated with this field of research, *fe-safe*® is utilized for fatigue life calculations. This software package, due to its implemented algorithms, is considered particularly suitable for depicting material behavior in the low cycle fatigue regime, most interesting for polymeric materials. Therefore, an interface was developed to handle manufacturing and structural simulation outputs and process them for fatigue analysis [4]. This offers the possibility to consider local fiber orientation without using additional composite materials modelling software, increasing the value of this work wherever such tools are not available.

2 FIBER ORIENTATION/ANISOTROPIC MATERIAL BEHAVIOR

Due to the occurring flow profile as well as the rheological behavior of the polymeric matrix material, adhesion between matrix and fiber material and fiber content, the fibers are oriented during the mold filling process, leading to a pronounced anisotropy. In Figure 1, the principal layered structure is shown.

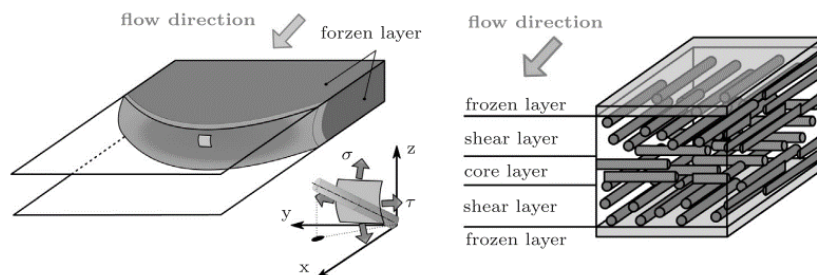


Figure 1: Flow-induced fiber alignment and resulting layered structure [5].

Different models are used to predict the fiber orientation for each element of a FE mesh. As a result, the fiber orientation is described by a symmetric second order 3 x 3 tensor derived by the use of orientation probability distribution functions $\psi(\mathbf{p})$, where $\mathbf{p}(\theta, \phi)$ describes the unit vector in a spherical coordinate system [4; 6; 7]:

$$\mathbf{p} = \begin{pmatrix} \sin \theta \cos \phi \\ \sin \theta \sin \phi \\ \cos \theta \end{pmatrix} \quad (1)$$

$$a_{ij} = \oint p_i p_j \psi(\mathbf{p}) dp = \begin{bmatrix} a_{11} & a_{12} & a_{13} \\ \dots & a_{22} & a_{23} \\ \text{SYM} & \dots & a_{33} \end{bmatrix} \quad (2)$$

The actual local fiber orientations with respect to the loading direction are provided by the tensor's eigenvectors λ , with the eigenvalues e giving the proportion of fibers in each direction (

Figure 2). The dependency of fatigue strength σ_a on fiber orientation can then be described by the model according to Gaier et al. [4; 8; 9]:

$$w_v = \frac{w_1 + w_2}{2} + \frac{w_1 - w_2}{2} \cdot \cos(2\alpha) \quad (3)$$

w is the material parameter, the subscripts 1, 2 and v describe the first and second principal direction and cutting plane normal and α is the angle between cutting plane normal and the fiber orientation. In the first and second principal direction, the fiber orientation proportions are assumed to be 1 and 0 respectively.

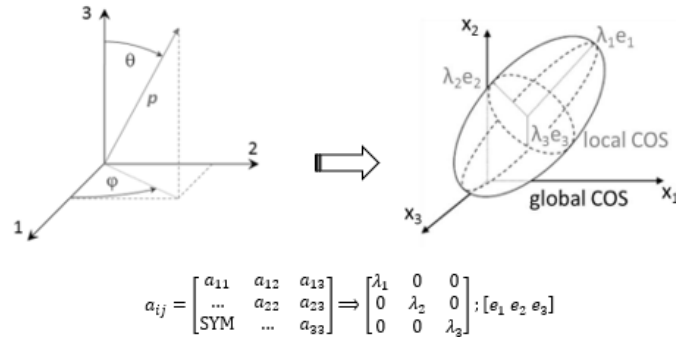


Figure 2: Schematic eigenvalue transformation of fiber orientation tensor [4].

3 LIFETIME ASSESSMENT

In a lifetime assessment, the calculated stress field due to an occurring load and the local material behavior are linked. In SFRPs microscopic cracks, originating from fiber ends acting as nuclei, steadily grow until merging to a macroscopic crack. Assuming that each load cycle causes the same amount of damage to the material, a linear damage accumulation such as Miner's rule [10] can be applied and the Woehler-curve can be described by equation **Fehler! Verweisquelle konnte nicht gefunden werden.** over the entire cycles-to-failure range [4].

$$N = N_D \cdot \left(\frac{\sigma_a}{\sigma_D} \right)^{-k} \quad (4)$$

Thereby, N is the number of cycles to failure by applied stress amplitude σ_a , σ_D is the endurance strength, or fatigue strength at $N_D = 10^6$ cycles and k is the slope of the curve.

By crack initiation under high loads, when local stresses exceed the material's yield strength, a linear correlation between stress and strain can no longer be assumed since the locally prevalent total strain amplitude includes a significant plastic deformation [11]. Equation **Fehler! Verweisquelle konnte nicht gefunden werden.** is no longer valid. The correlation between the strain amplitude ε_a and the

cycles to failure N must be characterized by a strain-life-curve; where instead of stress, the bearable strain amplitude is plotted against the cycles to failure on a single logarithmic scale [11; 12]:

$$\varepsilon_{a,t} = \varepsilon_{a,e} + \varepsilon_{a,p} = \frac{\sigma_f'}{E} \cdot (2N)^b + \varepsilon_f' \cdot (2N)^c \quad (5)$$

Thereby, σ_f' is the fatigue strength coefficient, E the elastic modulus, ε_f' the fatigue ductility coefficient, b the fatigue strength exponent and c the fatigue ductility exponent. $(\sigma_f'/E \cdot 2^b)$ and $(\varepsilon_f' \cdot 2^c)$ can be interpreted as the elastic and plastic share of the strain amplitude leading to failure after one reversal.

4 ESTABLISHED SIMULATION CHAIN

Material parameters of fiber-reinforced polymers are mainly influenced by fiber orientation, which is already determined in the manufacturing process. Therefore, the implementation of a process simulation into the simulation chain is of significant importance [4].

The established simulation chain (**Fehler! Verweisquelle konnte nicht gefunden werden.**) consists of the following steps:

- process simulation by means of injection molding to predict local fiber orientation
- structural simulation to estimate local stress-strain behavior
- data manipulation to derive local anisotropic material behavior, i.e., fatigue parameters from the above results and test data
- fatigue analysis to predict a component's life under defined cyclical loading

Data manipulation and calculation of local material parameters was performed using a self-developed *Python*TM program combining the calculated anisotropic stress field and predicted fiber orientations. Injection molding simulations to estimate process-induced fiber orientations were carried out. The results were mapped onto a mesh appropriate for subsequent structural analysis and provided in the form of fiber orientation tensors for each element. Concurrently, the model was built and pre-processed for static FE analysis [4].

4.1 Injection Molding Simulation

To predict flow induced fibre alignment during the injection moulding process, the applied simulation software *Moldex3D*[®] employs a modified anisotropic rotary diffusion model [13]. With its FEA interface, *Moldex3D*[®] offers the possibility to prepare results for implementation in subsequently applied software tools. A material homogenization can be performed, and the fiber orientation tensor can be computed and exported for each element. The homogenization method according to Mori-Tanaka [14] was used to account for local material behavior within the FE simulation, resulting in an anisotropic stress field. To account for anisotropic material behavior under fatigue loading due to fiber orientation, an influence factor was derived and “master Woehler-curves” were scaled based on Gaier's approach [4; 8; 9].

4.2 Determination of local material data

After a structure simulation in *ABAQUS*[®] where occurring stresses and deviations were calculated, the stress tensors consisting of six independent normal and shear stress components were read out. For comparison of predominant stresses and fiber orientations, a linear transformation of stress and fiber orientation tensors was conducted in a manner that shear stress components and non-diagonal elements of the fiber orientation tensor become zero. The eigenvectors represent the main directions of the fibers and the principal stresses respectively; with the eigenvalues giving the proportions of fiber orientation. An angle deviation between the eigenvectors corresponding to the largest eigenvalues (representing main fiber orientation and maximum principal stress respectively) can then be calculated. Since a fiber orientation proportion of 0 and 100 % cannot be achieved for a test specimen, a correction needs to be applied to avoid under- or over-estimation. Therefore, test results were extrapolated linearly to $\lambda = 1$. The correction factor f_α is calculated according to equation **Fehler! Verweisquelle konnte nicht gefunden werden.**), as illustrated in

Figure 3, left [4].

$$\frac{1}{f_\alpha} = \frac{3\lambda_l - 1}{2} \quad \text{for } 1/3 \leq \lambda_l \leq 1 \quad (6)$$

$$\frac{1}{f_\alpha} = 3\lambda_l - 1 \quad \text{for } 0 \leq \lambda_l \leq 1/3$$

Thereby, λ_l is the largest eigenvalue. Implementing the correction factor and rewriting equation **Fehler!** **Verweisquelle konnte nicht gefunden werden.** exemplarily for the stress amplitude σ_a gives:

$$\sigma_a = \frac{\sigma_{a,long} + \sigma_{a,trans}}{2} + \frac{1}{f_\alpha} \cdot \frac{\sigma_{a,long} - \sigma_{a,trans}}{2} \cdot \cos(2\alpha) \quad (7)$$

Using this approach, cyclical material data for fatigue analysis can be provided for each location in the part by interpolation between given data sets, preliminary determined by cyclical tension and compression tests longitudinally and transversely to fiber orientation.

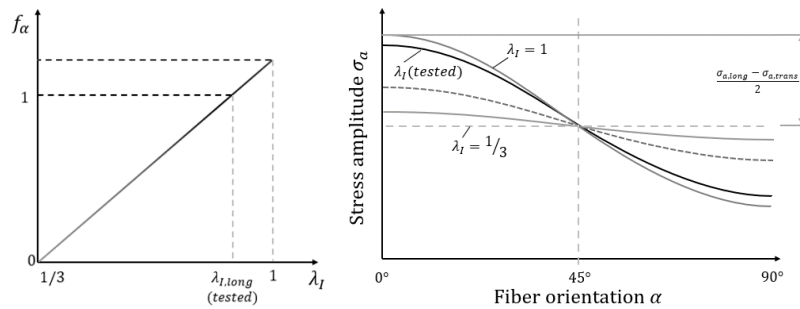


Figure 3: Extrapolation of the correction factor (left) and effect on interpolation of material parameters (right).

In

Figure 4, the scheme of the developed interface is outlined. The *.inp file contains the mesh and material information, which provides the basis for the anisotropic FE analysis. The *.o2d file contains the fiber orientation tensors for each element, retrieved from the injection molding simulation. The latter one is directly used alongside the stress tensors read from the FE output (*.odb) to calculate the correction factor for each node. Then, in conjunction with a provided data set, the local material data is derived. This data is written to a specific file format (*.npd) which can be imported to *fe-safe*[®] [4].

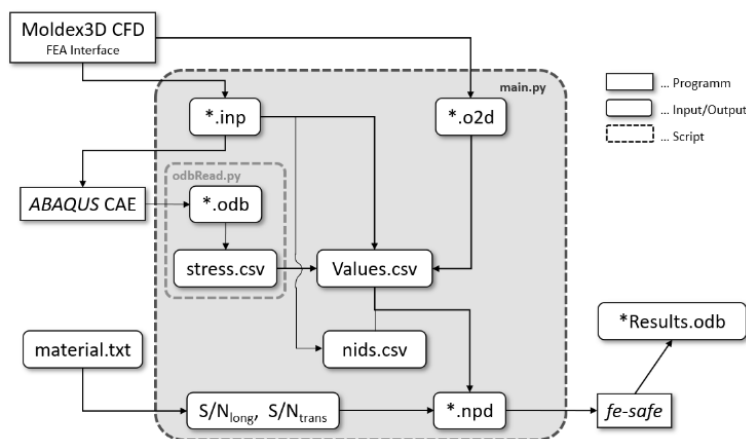


Figure 4: Scheme of the developed interface.

4.3 Fatigue analysis

fe-safe[®] allows for stress- as well as strain-based fatigue life calculation, supposed that appropriate material data is provided. For predicting damage by cyclical loading, different damage parameters and mean stress correction methods are implemented depending on the applied algorithm.

For the evaluation of the established simulation chain, a short fiber reinforced semi-aromatic polyamide-blend with a fiber content of 50 % by weight (AKROLOY[®] PA GF50, AKRO-PLASTIC GmbH, Niederrissen, Germany) is investigated. Normalized fatigue test results in terms of Woehler-curves are shown in Figure 6. Based on these studies, fatigue material data were derived by employing a material generator developed by Primetzhofer [15]. For reasons of simplification, it was assumed that the slope of the Woehler-curve k is independent of the stress ratio R and the fiber direction (longitudinally/transversely). Besides, an extensive literature review on fatigue properties of polymers was conducted [16-19] and a dataset was determined (Table 1) comparing derived and literature data [4]. Using this data, different stress- and strain-based algorithms and mean stress correction methods were evaluated.

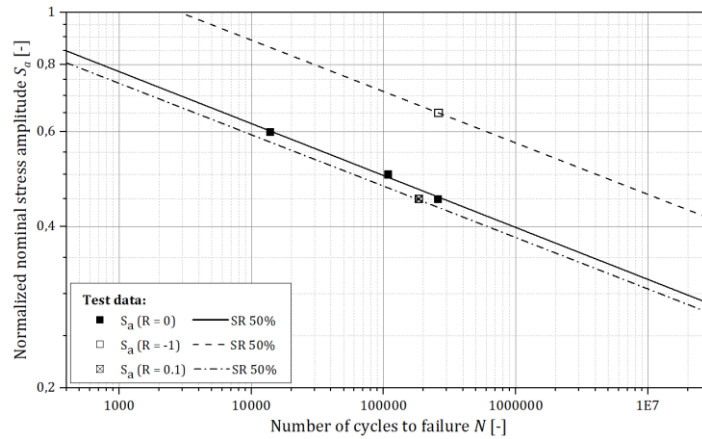


Figure 5: Normalized Woehler-curves for standardized test specimen made from AKROLOY[®] PA GF50. $T = RT$, $f = 5$ Hz. SR = survival rate

	E [MPa]	σ_D ($R=-1$)	σ_D ($R=0$)	k	σ'_f
long.	18450	67.6	31.0	10.4	379
trans.	12250	45.0	21.0	10.4	252
	ε'_f	b	c	K'	n'
long.	0.07	-0.1	-0.6	421	0.167
trans.	0.05	-0.1	-0.6	265	0.167

Index: K' , n' = Neuber Parameters for plasticity correction

Table 1: Material data set used for fatigue simulation

5 RESULTS AND VALIDATION

5.1 Standardized Test Specimen

The simulation was set up corresponding to fatigue tests under pure tension ($R = 0$) and tension-compression ($R = -1$). Loads causing normalized nominal stresses of 0.4, 0.45, 0.5, 0.6 and 0.65, respectively, were applied. Results obtained by specimen tests and simulations are in good accordance, but stress-based algorithms under-estimate damage while strain-based ones tend to be a little too conservative (Figure 6 and Figure 7). Stresses obtained by the simulations are not the highest ones exhibited, but refer to the nodes showing the lowest number of cycles to failure. For all tested algorithms, these nodes are found to be in the same region of the specimen.

Analyzing results for different loading conditions and algorithms states that taking anisotropic material behavior, mean stress and plasticity correction into account is essential. Comparing results for stress- and strain-based calculations also emphasizes the fact that the failure criterion differs between the algorithms. In the stress-life curve, the final number of cycles refers to the rupture of the specimen, while strain-life corresponds to crack initiation.

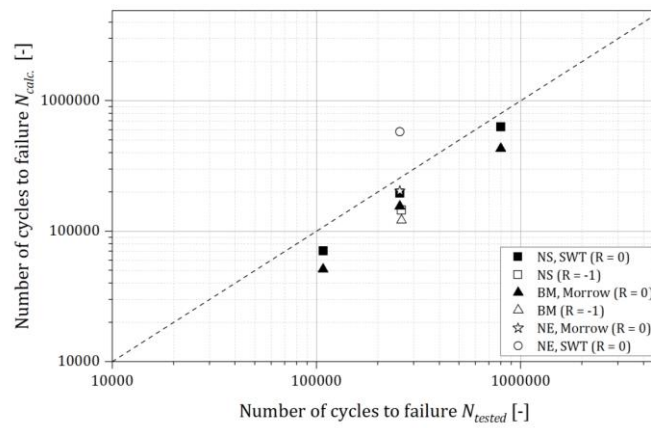


Figure 6: Number of cycles to failure obtained by specimen tests vs. simulation.

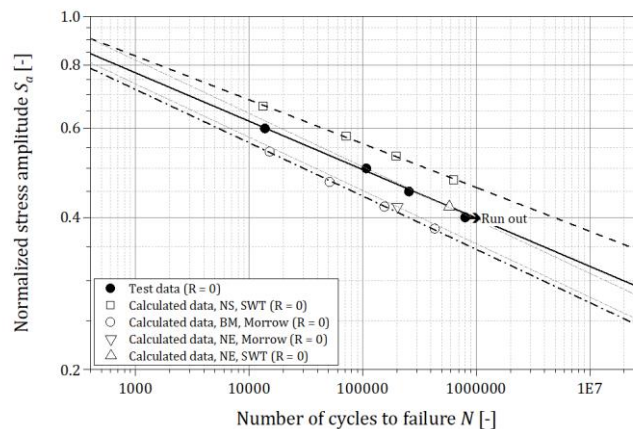


Figure 7: Comparison of Woehler-curves obtained from specimen tests ($T = RT$, $f = 5$ Hz) and simulations.

Index: NS = Normal Stress algorithm (only stress data from FE analysis), NE = Normal Strain algorithm (stress and strain data from FE analysis), BM = Brown-Miller algorithm (stress and strain data from FE analysis), R = stress ratio, SWT = Smith-Watson-Topper mean stress correction.

5.2 Structural Part

Fatigue simulations were performed under tension ($R = 0$) at a specified load level. Figure 8 depicts a full load cycle by combining FE models for three different load directions. A cross sectional cut in the x-z-plane (Figure 9) shows the fiber orientation in all directions, predicted by the process simulation. An inhomogeneous fiber orientation distribution, with the majority of the fibers aligned in z-direction, which corresponds to the main direction of the melt flow during injection molding, can be observed.

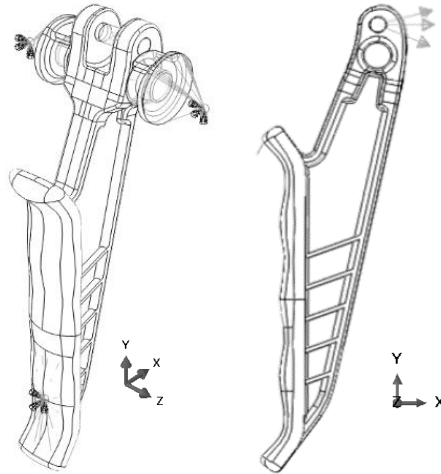


Figure 8: FE model of the dispenser trigger arm illustrating boundary conditions and couplings for bearing shells (left) and applied loads (right).

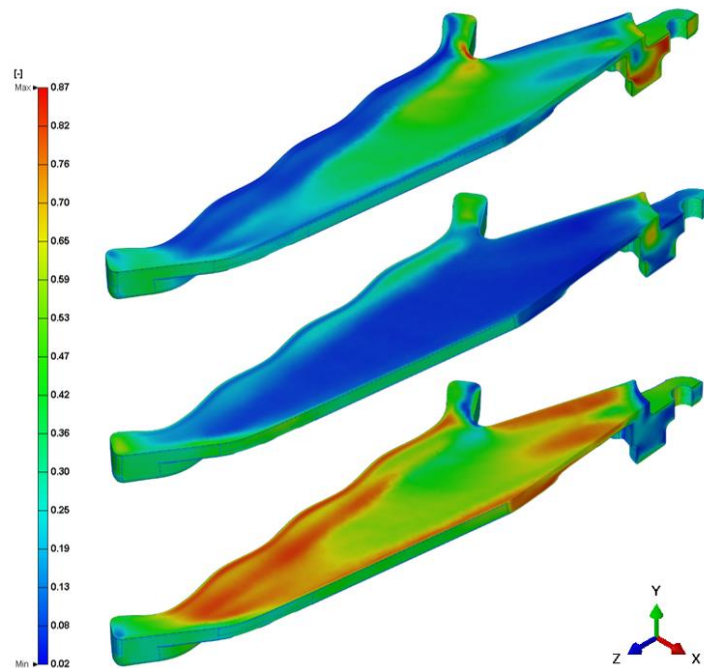


Figure 9: Cross-sectional cuts in the x-z-plane showing the fiber orientation distribution in x- (top), y- (middle) and z-direction (bottom).

In

Figure 10, left, the von Mises equivalent stress, showing elevated stresses at the radius of the bearing surface, is depicted. As fiber orientation has a big impact on material strength, an exact prediction of the fiber orientation in these highly stressed areas is of significant importance. **Fehler! Verweisquelle konnte nicht gefunden werden.**, right shows the number of cycles to failure for the dispenser trigger arm under tensile cyclic loading ($R = 0$). As expected, the lowest number of cycles to failure can be found at the radii of the bearings. The number of fibers oriented in load-direction decreases in this area due to the melt flow. A fractured part, verifying the designated area of failure is depicted in Figure 11. Locations of crack initiation and residual fracture are highlighted. The simulation results for both stress- and strain-based calculations (

Table 2) seem to provide a good correlation with empirical values. However, it must be noted that simulation results always apply only for one node in the FE mesh. The number of cycles to failure obtained in direct proximity to this node exceed the lifetime by around 20 percent. This also suggests that the quality and refinement of the FE mesh influence the obtained fatigue results.

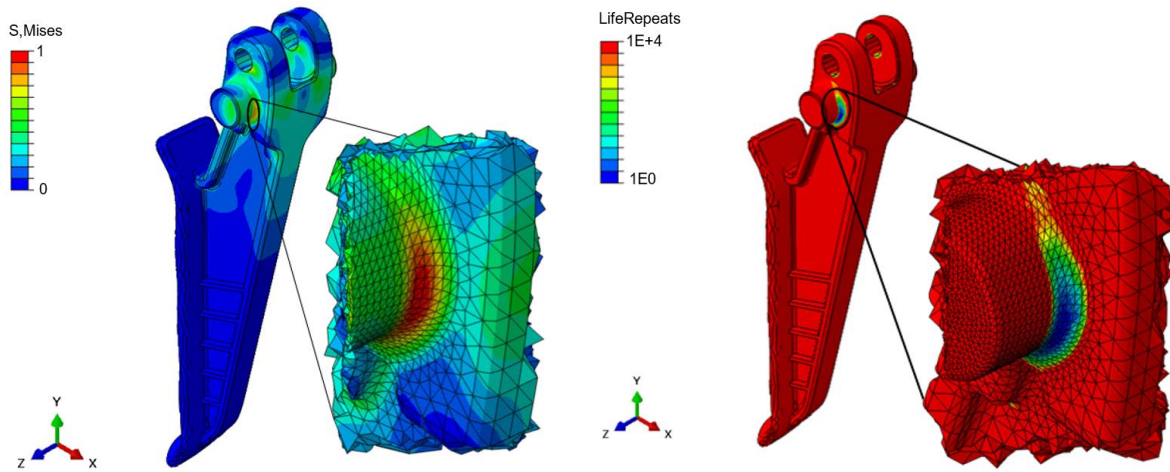


Figure 10: Normalized von Mises equivalent stress caused by a tensile load (left), normalized number of cycles to failure under tensile cyclic loading at $R = 0$ (right).



Figure 11: Fracture after cyclic loading.

	Dataset	R	Algorithm	MSC	N_{calc}/N_{test} [-]
1	σ	0	NS	SWT	0.52 – 2.08
2	σ/ε	0	BM	Morrow	0.95 – 3.78

Table 2: Results of fatigue simulations at different loading conditions,
 Material: AKROLOY PA GF 50[®]

Index: σ = only stress data from FE analysis, σ/ε = stress and strain data from FE analysis, R = stress ratio, NS = Normal Stress, BM = Brown-Miller, MSC = applied mean stress correction algorithm, N = Number of cycles to failure, SWT = Smith-Watson-Topper.

ACKNOWLEDGEMENTS

This research work was performed at the Chair of Materials Science and Testing of Polymers at the Montanuniversitaet Leoben in collaboration with the Polymer Competence Center Leoben GmbH (PCCL, Austria) with contribution by medmix Switzerland AG. The PCCL is funded by the Austrian Government and the State Governments of Styria, Lower and Upper Austria.

REFERENCES

- [1] C. Guster “Ansätze zur Lebensdauerberechnung von kurzglasfaserverstärkten Polymeren”, Dissertation Montanuniversität Leoben, Leoben, AT, 2009
- [2] C. Guster, G. Pinter, A. Mösenbacher et al. “Evaluation of a Simulation Process for Fatigue Life Calculation of Short Fibre Reinforced Plastic Components” *Procedia Engineering*, 10, pp. 2104–2109, 2011
- [3] A. Primetzhofer, G. Stadler, G. Pinter et al., Data set determination for lifetime assessment of short fibre reinforced polymers, *Journal of plastics technology*, **15** (1), 2019
- [4] D. Kaylani, Stress- and Strain-based Fatigue Life Calculation for Short Fiber Reinforced Polymers by Use of fe-safe, Master’s Thesis Montanuniversität Leoben, Leoben, AT (2022)
- [5] A. Primetzhofer, G. Stadler, G. Pinter, Lifetime assessment of anisotropic materials by the example of short fibre reinforced plastic, *International Journal of Fatigue*, **120**, 2019, pp. 294–302
- [6] J. Jansson, T. Gustafsson, K. Salomonsson et al., An anisotropic non-linear material model for glass fibre reinforced plastics, *Composite Structures*, **195**, 2018, pp. 93–98
- [7] R. Zheng, R. I. Tanner, X. Fan, *Injection Molding*, Integration of Theory and Modeling Methods, Springer, Berlin, Heidelberg, 2011
- [8] C. Gaier, H. Dannbauer, A. Werkhausen et al., Fatigue Life Prediction of Short Fiber Reinforced Plastic Components, *Proceedings of the 8th Annual Automotive Composites Conference and Exhibition (ACCE 2008)*, Troy, Michigan, USA, SPE Automotive and Composites Division, 2008, pp. 1189–1197
- [9] C. Gaier, H. Fleischer, C. Guster et al., Einfluss von Faserorientierung, Temperatur und Feuchtigkeit auf das Ermüdungsverhalten von kurzfaserverstärkten Thermoplasten, *Materials Testing*, **52** (7-8), 2010, pp. 534–542
- [10] M. A. Miner, Cumulative Damage in Fatigue, *Journal of Applied Mechanics*, **12**, 1945, pp. 59–64

- [11] E. Haibach, *Betriebsfestigkeit*, Verfahren und Daten zur Bauteilberechnung, Springer, Berlin, Heidelberg, 2006
- [12] Y. Lee, M. E. Barkey, *Strain-Based Uniaxial Fatigue Analysis*, Metal Fatigue Analysis Handbook. Practical Problem-solving Techniques for Computer-Aided Engineering, Butterworth-Heinemann. Waltham MA, 2012, pp. 215–252
- [13] CoreTech System Co., Ltd., *Moldex3D Help*, 2020
<http://support.moldex3d.com/2020/en/index.htm>
- [14] T. Mori, K. Tanaka, Average stress in matrix and average elastic energy of materials with misfitting inclusions, *Acta Metallurgica*, **21** (5), 1973, pp. 571–57
- [15] A. Primetzhofer, Erweiterte Lebensdauerabschätzung für Bauteile aus kurzglasfaserverstärkten Kunststoffen, Dissertation Montanuniversität Leoben, Lehrstuhl für Allgemeinen Maschinenbau, Leoben, AT, 2018
- [16] A. N. Abood, A. H. Saleh, A. A. Ali et al., Low cycle fatigue of different polymer types PA, PVC and POM, *Elixir Mech. Engg.*, **38**, 2011, pp. 4154–4156
- [17] A. Bernasconi, F. Cosmi, D. Taylor, Analysis of the fatigue properties of different specimens of a 10% by weight short glass fibre reinforced polyamide 6.6, *Polymer Testing*, **40**, 2014, pp. 149–155
- [18] A. Bernasconi, P. Davoli, A. Basile et al., Effect of fibre orientation on the fatigue behaviour of a short glass fibre reinforced polyamide-6, *International Journal of Fatigue*, **29** (2), 2007, pp. 199–208
- [19] S. R. Mellot, A. Fatemi, Fatigue behavior and modeling of thermoplastics including temperature and mean stress effects, *Polymer Engineering & Science*, **54** (3), 2014, pp. 725–738